A novel model for calculating the inter-electrode capacitance of wedge-strip anode

Airong Zhao and Qiliang Ni'

Citation: Review of Scientific Instruments **87**, 043101 (2016); doi: 10.1063/1.4944940
View online: http://dx.doi.org/10.1063/1.4944940
View Table of Contents: http://aip.scitation.org/toc/rsi/87/4
Published by the American Institute of Physics

A novel model for calculating the inter-electrode capacitance of wedge-strip anode

Airong Zhao[1,2] and Qiliang Ni[1,a)]
[1]*Changchun Institute of Optics, Fine Mechanics and Physics, Chinese Academy of Sciences, Changchun 130033, China*
[2]*University of Chinese Academy of Sciences, Beijing 10039, China*

(Received 20 September 2015; accepted 16 March 2016; published online 1 April 2016)

The wedge strip anode (WSA) detector has been widely used in particle detection. In this work, a novel model for calculating the inter-electrode capacitance of WSA was proposed on the basis of conformal transformations and the partial capacitance method. Based on the model, the inter-electrode capacitance within a period was calculated besides the total inter-electrode capacitance. As a result, the effects of the WSA design parameters on the inter-electrode capacitance are systematically analyzed. It is found that the inter-electrode capacitance monotonically increases with insulated gap and substrate permittivity but not with the period. In order to prove the validation of the model, two round WSAs were manufactured by employing the picosecond laser micro-machining technology. It is found that 9%–15% errors between the theoretical and experimental results can be obtained, which is better than that obtained by employing ANSYS software. © *2016 AIP Publishing LLC.* [http://dx.doi.org/10.1063/1.4944940]

I. INTRODUCTION

Photon-counting imaging detectors consisting of microchannel plate (MCP) and a position-sensitive anode have been widely used in nuclear physics and particle detection.[1–4] As a position sensitive anode, the three-electrode wedge strip anode (WSA) is well known for its high position resolution and a rather simple electronics; thus, it has been used in many fields.[5–8] Moreover, there are many transformations of WSA for more appropriate applications.[9–12]

For a WSA detector, the spatial resolution is affected by the electronic noise and the charge division noise.[13] The electronic noise mainly arising from its charge-sensitive preamplifier becomes the only noise source in the induced charge mode. In this case, the electrons ejected from the MCP stack are incident on a resistive layer instead of being collected by the metal WSA directly;[14] as a result, the charge pulse is induced onto the metal WSA. Furthermore, the noise only increases with the rise of the WSA inter-electrode capacitances. Because the WSA inter-electrode capacitances are related to its design parameters, the accurate relationship between both is quite helpful for one to design a WSA with low electronic noise. Although computer simulation technique such as using ANSYS software in finite element method can also calculate the inter-electrode capacitances,[15] this technique can only give the total inter-electrode capacitances among three electrodes, and it cannot let one know how the design parameters influence the inter-electrode capacitances. Therefore, a new physical model is necessary to study the WSA inter-electrode capacitances.

So far, two models for calculating the WSA inter-electrode capacitances have been reported. One was developed by Allington and Schwarz in 1984[16] and the other was developed by Thornton in 1987.[17] The former method is capable of calculating the total capacitance among the three electrodes of the WSA. In this model, the inter-electrode capacitances are divided into two parts. One is the line capacitor that is formed by the edge of the neighboring electrodes and the insulated gap. The other is the strip capacitor that is contributed by the area of the electrodes. The latter model employs the mean width values of the electrodes and regards two electrodes as one while estimating the capacitance formed by the third electrode when calculating the period capacitance. The total capacitance in this model is N times the period capacitance, where N is the number of periods. However, it is found that both methods do not allow one to calculate the capacitance between any two of the three electrodes within a period, while it is of great importance to understand the characteristic of any inter-electrode capacitances for a stringent study on the principle of WSA design and the electronic noise.

In this work, a novel model for obtaining the total inter-electrode capacitance of the WSA by calculating the capacitance between any two of the three electrodes was proposed. Under some reasonable approximations and presumptions, the model transfers the calculation of inter-electrode capacitances into the calculation of electrode capacitances against ground. It takes the variation of electrodes' width into account and therefore makes the calculated results more accurate. Based on the model, the WSA structure parameter's effect on the anode inter-electrode is analyzed. The optimized scheme is proposed to design the WSA with less electronic noise.

a)Author to whom correspondence should be addressed. Electronic mail: qiliangni@qq.com

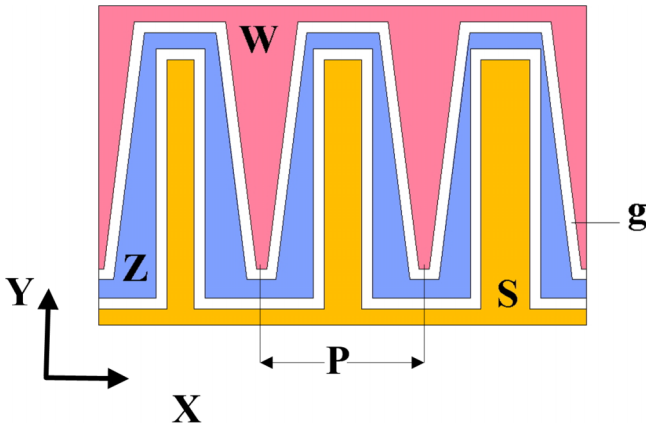

FIG. 1. A schematic diagram of the WSA with three electrode elements in each period.

II. THE MODEL OF THE WSA INTER-ELECTRODE CAPACITANCE

The WSA operates by dividing the emergent electron cloud from a MCP stack into several electrodes. Figure 1 shows the typical anode design with three electrodes in each period. Where g is the width of the insulation gap, P is the period and W (wedge), S (strip), and Z (zig-zag) are three parts separated by two insulated gaps. Generally, a rectangular WSA consists of many periods with the same size. For each period, S is a rectangle, W is an inverted isosceles trapezoid with the bottom width equal to a half of period, and Z is the area between W and S. Thus, each period has two parts of Z, both symmetrically arranging on S two sides and connecting together in tandem. The strip width of S part increases linearly across the anode area in the horizontal direction, while the wedge width of W part increases linearly in the perpendicular direction. Consequently, the charges deposited on the S and W electrodes linearly vary along X and Y coordinates.

Fig. 2 shows the cross section of the WSA within one period, where W, Z, and S are assumed to connect to the potential of +V, –V, and +V, respectively. Based on the theory of electrostatics, there must exist equipotential lines with V = 0 between the neighboring electrodes. So the capacitances between Z, W, and S due to the insulation gaps can be simplified as the model shown in Fig. 3 by assuming the following approximations:[18]

(a) electrode thickness is negligible in comparison with its width;
(b) the length of the electrode must be much greater than its width so that the electrode can be considered as infinite long;

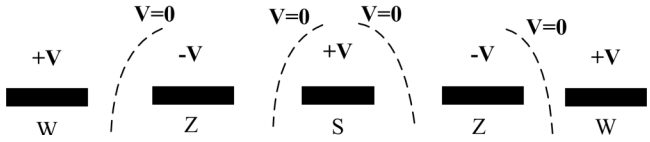

FIG. 2. A cross section diagram of the WSA within a period.

(c) capacitance coupling only exists between neighboring electrodes such as Z and S, Z and W, within the same period; thus, there is no coupling between W and S in the same period because both are separated by Z electrode.

In Fig. 3, C_{WZ} is the unit length capacitance between Z and W in a period in Y direction. C_{ZS} is the unit length capacitance between Z and S in a period in Y direction. C_S and C_W is a half of the unit length capacitance of S and W relative to the ground in a period in Y direction for the symmetry reason. C_{Z1} and C_{Z2} are parts of the unit length capacitances of Z with respect to the ground in a period in Y direction. Below are approximations of C_{Z1}, C_{Z2},

$$C_{Z1} = [s/(s+w)]\,C_z, \tag{1}$$
$$C_{Z2} = [w/(s+w)]\,C_z, \tag{2}$$

where s and w are the widths of S and W adjacent to the same Z, and C_Z is the unit length capacitance of Z with respect to the ground. As is shown in Fig. 3, one can see that Z, W, and S are series connected. Therefore, the unit length capacitance between Z, S, and W in a period in Y direction can be expressed as follows:

$$C_{ZS} = 2\left(\frac{C_{Z1}C_S}{C_{Z1}+C_S}\right), \tag{3}$$
$$C_{ZW} = 2\left(\frac{C_{Z2}C_W}{C_{Z2}+C_W}\right), \tag{4}$$
$$C_{SW} = \frac{C_{ZS}C_{ZW}}{C_{ZS}+C_{ZW}}. \tag{5}$$

Since unit length capacitances along Y direction in one period are series connected, the period capacitance, which is defined as the total capacitance in one period, can be obtained by integrating C_{zs}, C_{zw}, and C_{sw} along Y direction, respectively. The total inter-electrode capacitances between Z, S, and W are the sum of the period capacitances between Z, S, and W for all periods, which can be expressed as follows:

$$C_{total-ZS} = \sum_1^N \int_0^L C_{ZS} = 2\sum_1^N \int_0^L \left(\frac{C_{Z1}C_S}{C_{Z1}+C_S}\right), \tag{6}$$

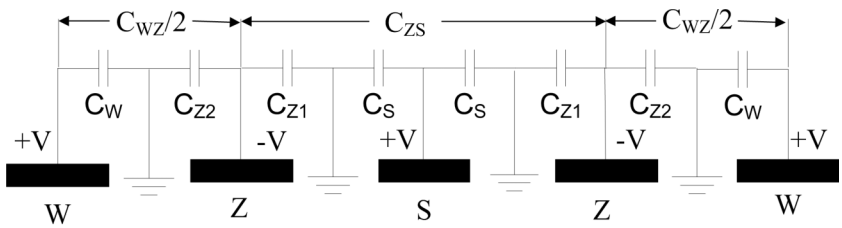

FIG. 3. A simplified model of inter-electrode capacitance between Z, W, and S within a period.

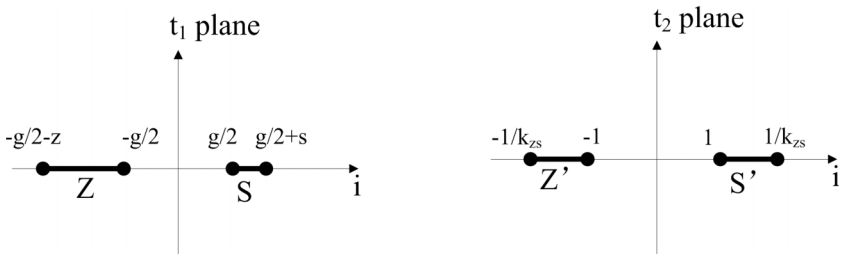

FIG. 4. A transformation of the asymmetric electrode elements Z and S into symmetric ones.

$$C_{total-ZW} = \sum_{1}^{N} \int_{0}^{L} C_{ZW} = 2 \sum_{1}^{N} \int_{0}^{L} \left(\frac{C_{Z2} C_W}{C_{Z2} + C_W} \right), \quad (7)$$

$$C_{total-SW} = \sum_{1}^{N} \int_{0}^{L} C_{SW} = 2 \sum_{1}^{N} \int_{0}^{L} \left[\frac{C_{Z1} C_{Z2} C_S C_W}{C_{Z1} C_S (C_{Z2} + C_W) + C_{Z2} C_W (C_{Z1} + C_S)} \right], \quad (8)$$

where N is the period number and L is the length of the electrode.

III. COMPUTATION FOR THE INTER-ELECTRODE CAPACITANCE

It is difficult to get the position of the equipotential lines with V = 0 shown in Fig. 2, because the width of Z and W electrode elements continuously changes along the Y direction. This makes it hard to calculate the values of C_S, C_W, C_{Z1}, and C_{Z2}. To ease the calculation, transformations are taken to make the equipotential lines perpendicular to the X-Y plane. Taking S and Z as example, in order to make the equipotential lines with V = 0 be perpendicular to the X-Y plane, the distribution of electric field lines around S and Z should be symmetric. This needs to transform asymmetric electrode elements into symmetric ones with the same width by using conformal mapping method.[19] Fig. 4 shows how this transformation is implemented from t_1 plane to t_2 plane.

In Fig. 4, the t_1 plane gives the asymmetric electrode elements of S and Z under Cartesian coordinate system in which the middle position of the inter-electrode insulation gap is taken as the ordinate origin, where the variables z, s, and g in the t_1 plane represent the width of electrode Z, S, and the insulated gap, respectively. The t_2 plane gives symmetric electrodes of Z′ and S′ with the same width of ($1/k_{zs}$ - 1), and the gap between Z′ and S′ is set as 2 mm.

The conformal translation from t_1 plane to t_2 plane is a bilinear transformation, and the translation formula is as follows:

$$t_1 = t_0 + \lambda / (t_2 + \upsilon), \quad (9)$$

where t_0, λ, and ν are undetermined constants. By substituting the coordinates in t_1 and t_2 plane into formula (9), the value of k_{zs} in t_2 plane can be expressed as follows:[19]

$$k_{zs} = \frac{(z + s + g)\, g}{2zs + (z + s + g)\, g + 2\sqrt{z^2 s^2 + zsg\,(z + s + g)}}. \quad (10)$$

By using the above bilinear transformation, the equipotential line for V = 0 between Z and S can be mapped into the line that is perpendicular to i axis in t_2 plane and positioned in the middle of Z′ and S′. In this case, C_S and C_{Z1} can be calculated by employing the conformal transformation. Fig. 5 shows the transformation from A plane to E plane to calculate the capacitances between the electrode elements with respect to the ground potential.[18]

Here takes C_{Z1} as an example. Plane A is used to define the physical domain, where the distance from point A_1 to point A_2 represents the width of Z′ that is relative to C_{Z1}, and the line determined by points A_3 and A_4 represents the ground equipotential line. Therefore, the width D of Z′ and the coefficient h can be expressed by

$$D = \frac{1}{k_{ZS}} - 1, \quad (11)$$

$$h = \frac{s}{s + w}. \quad (12)$$

Plane A can be transformed into plane B by using the function

$$B = \frac{1}{k} \sin\left(\frac{2\pi}{\lambda} A\right), \quad (13)$$

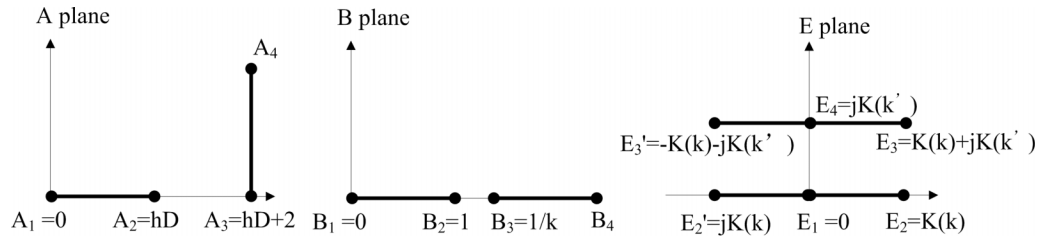

FIG. 5. Transformations from A plane to E plane for calculating C_{Z1}.

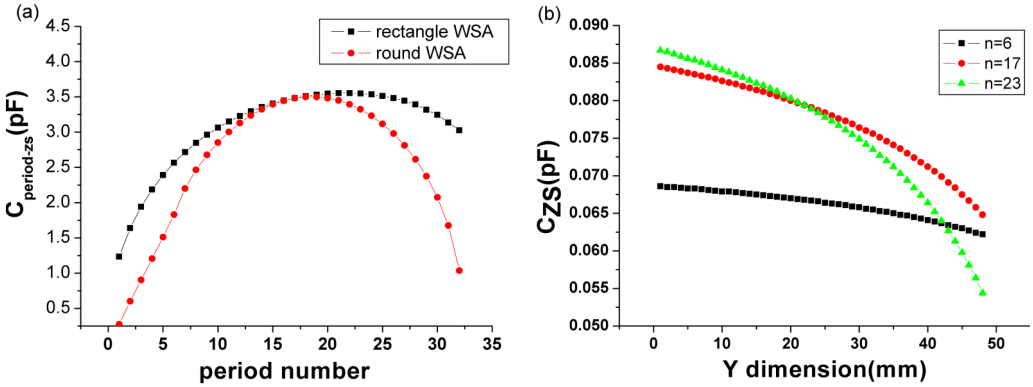

FIG. 6. (a) The period capacitance against the period number for different shapes of WSA with the total period number N = 32; (b) the variation of unit length capacitance along Y direction in the 6th, 17th, and 23rd periods for a rectangular WSA.

where the parameter k can be expressed by

$$k = \sin\left(\frac{\pi}{2hD+4}hD\right). \tag{14}$$

Plane B can be transformed into plane E by using Schwarz-Christoffel transformation[20] to get the capacitance,

$$C_{Z1} = 2\varepsilon_{eff}\frac{K(k)}{K(k')}, \tag{15}$$

where K(k) is the elliptic integral of the first kind and k′ can be expressed by

$$k' = \sqrt{1-k^2}. \tag{16}$$

ε_{eff} is the effective permittivity of the anode, which can be expressed by

$$\varepsilon_{eff} = \varepsilon_0(\varepsilon+1)/2, \tag{17}$$

ε_0 is the vacuum permittivity and ε is the relative permittivity of the substrate.

In the same way, one can calculate the values of C_S, C_W, and C_{Z2},

$$C_s = \varepsilon_{eff}\frac{K(k_s)}{K(k_s')}, k_s = \sin\left[\frac{\pi}{2}\left(\frac{1-k_{zs}}{1+k_{zs}}\right)\right], \tag{18}$$

$$C_w = \varepsilon_{eff}\frac{K(k_w)}{K(k_w')}, k_w = \sin\left[\frac{\pi}{2}\left(\frac{1-k_{zw}}{1+k_{zw}}\right)\right], \tag{19}$$

$$C_{z2} = \varepsilon_{eff}\frac{K(k_{z2})}{K(k_{z2}')}, k_{z2} = \sin\left[\pi\left(\frac{1-k_{zw}}{1+k_{zw}}\right)\left(\frac{w}{s+w}\right)\right], \tag{20}$$

where

$$k_{zw} = \frac{(z+w+g)g}{2zw+(z+w+g)g+2\sqrt{z^2w^2+zwg(z+w+g)}}. \tag{21}$$

IV. RESULTS AND DISCUSSIONS

A. Calculated results

Normally, the MCP stack used in a WSA detector has a round shape; thus, the round WSA is preferred. Fig. 6(a) shows the calculated period capacitance between Z and S as a function of the period number for a round and rectangular WSA with same design parameters of WSA I shown in Table I. To study the variation of the unit length capacitance in different period, the unit length capacitance, C_{ZS}, along Y direction for different periods for a rectangular WSA is also given in Fig. 6(b).

As can be seen from Fig. 6(a), the round WSA has a smaller period capacitance than the rectangular one due to the smaller area. For the round WSA, the capacitance increases linearly from 0.25 pF to 2.5 pF for periods ranging from 1 to 7 and then rise up slowly to reach the maximum at the 17th period. The capacitance starts to drop when period number is larger than 17, and it quickly drops to 1 pF at the 32nd period. However, for the rectangular WSA, the capacitance reaches the maximum at period 20 but does not drop quickly after period 20 and only reduce about 0.5 pF at the 32nd period. For the unit length capacitance C_{ZS}, it always decreases monotonically along Y direction for every period. The larger the period number is, the faster the decrement of C_{ZS} is. These characteristics of the capacitance are quite helpful for one to understand and design the WSA.

In addition, the above model can also be used to analyze the effect of the WSA design parameters on the total inter-electrode capacitance, for instance, the total inter-electrode capacitance between S and Z electrode $C_{total\text{-}ZS}$. Fig. 7 shows the effect of the widths of the insulation gap and the period on the $C_{total\text{-}ZS}$. Here, the design parameters of the anode are the same with the WSA I that shown in Table I. As can be seen, the total capacitance reduces linearly with the increase of the width of the insulation gap. However, for different widths of period, the total capacitance increases first when the period

TABLE I. All design parameters for WSA I and WSA II.

Anodes	WSA I	WSA II
Width of the period (P)	1.5 mm	1 mm
Total number of the period (n)	32	44
Diameter of the anode (D)	48 mm	44 mm
Width of the insulation gap (g)	0.06 mm	0.03 mm
Relative permittivity of the substrate (ε)	4.3	4.3
Width of the first S electrode (s_0)	0.02 mm	0.01 mm
Increment of the S electrode (δs)	0.02 mm	0.01 mm
Bottom width of the W electrode (w_0)	0.69 mm	0.47 mm

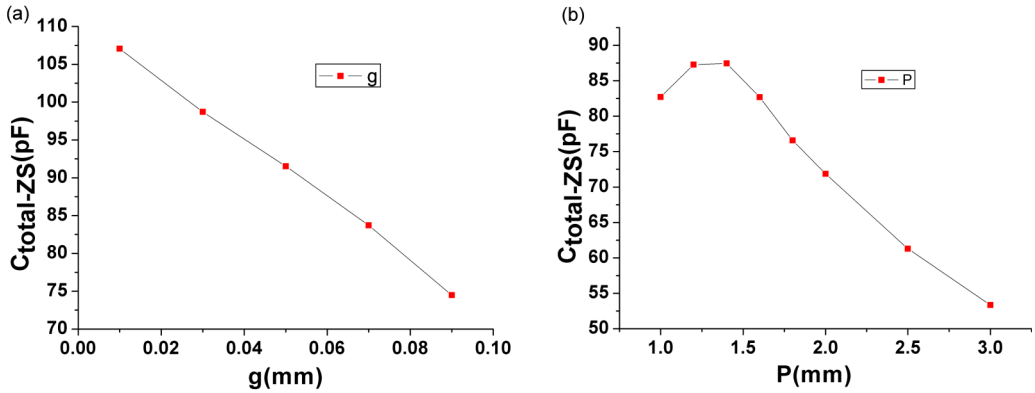

FIG. 7. $C_{total\text{-}SZ}$ as a function of g (a) and P (b).

width increases from 1 mm to 1.5 mm and then reduces almost linearly when the period width increases from 1.5 mm to 3 mm. Apparently, there exists a maximum value for the total capacitance when the period width changes. In general, Fig. 7 shows that the width of the insulation gap has a greater influence on $C_{total\text{-}ZS}$ than the period width. The above results are consistent with the conclusion obtained by Allington and Schwarz.[16]

B. Optimization of the WSA

In order to achieve a less electronic noise and a better spatial resolution, the optimal anode configuration is proposed as follows.

1. Maximize the pitch width

Fig. 7(b) shows that a total capacitance does not change monotonically with period width. There exists a maximum value for the total capacitance when the period width changes. According to the theory proposed by Allington and Schwarz in 1984,[16] the spatial resolution is almost in inverse proportion to the period width. In addition, too small period including four insulated gaps can lead to bad image linearity. So maximizing the pitch width if the charge cloud is suitable can decrease the total inter-electrode capacitance, thus improve the spatial resolution.

2. Minimize the first strip width of the S electrode

According to Fig. 6(a), we know that a minimum and a maximum capacitance value exist among the period capacitances. The minimum capacitance is determined by the first strip width of the S electrode. So the width of the first strip should be as small as possible when processing technique for anode fabrication can satisfy this demand.

3. Design the shape of WSA

As we all know, the MCP stack used in a WSA detector has a round shape, which is designed by cutting the rectangular WSA with a circle. Fig. 6(b) shows that the unit length capacitance always decreases monotonically along Y direction in a period. That is to say, one can get a less capacitance by reducing lower part and reserving upper part of the rectangular WSA when cutting it. This method has been used for the WSA design by Grasso *et al.* in 2013.[9]

4. Maximize the insulation gap

Fig. 7(a) shows that the width of the insulation gap has a great influence on the total inter-electrode capacitance, so maximize the insulation gap under the condition that the image linearity is fine.

5. Appropriate substrate

The substrate should have as small permittivity as possible; at the same time, it should also have enough hardness.

C. The estimation of calculated capacitances by experiment

In order to prove the validation of the developed method, two round WSAs were fabricated on a glass substrate ($\varepsilon = 4.3$) with a thickness of 2 μm Al film deposited on its surface by using the laser micro-machining technique. Fig. 8 shows the photographs of two anodes, and their design parameters are listed in Table I. For comparison, ANSYS software was also employed to calculate the total inter-electrode capacitances.

Referred to the calculation method with ANSYS software proposed by Xing *et al.*,[15] the total inter-electrode capacitances were got by following processes:

(a) Set electric module as ANSYS working conditions.
(b) Build a WSA model by UniGraphics software and import it to the ANSYS software.
(c) Define materials properties and mesh the WSA into element size of 10 μm.
(d) Delimit the boundary conditions for the WSA by applying excitation voltage to the anode center.
(e) Calculate the capacitance by "CMATRIX" command.

Tables II and III illustrate the comparison of the measured inter-electrode capacitances with the calculated values and simulated ones by the ANSYS software for WSA I and WSA II, respectively.

Tables II and III show that the simulated capacitances are about 22% larger than those of experimental values. However, the calculated capacitances based on our model are much

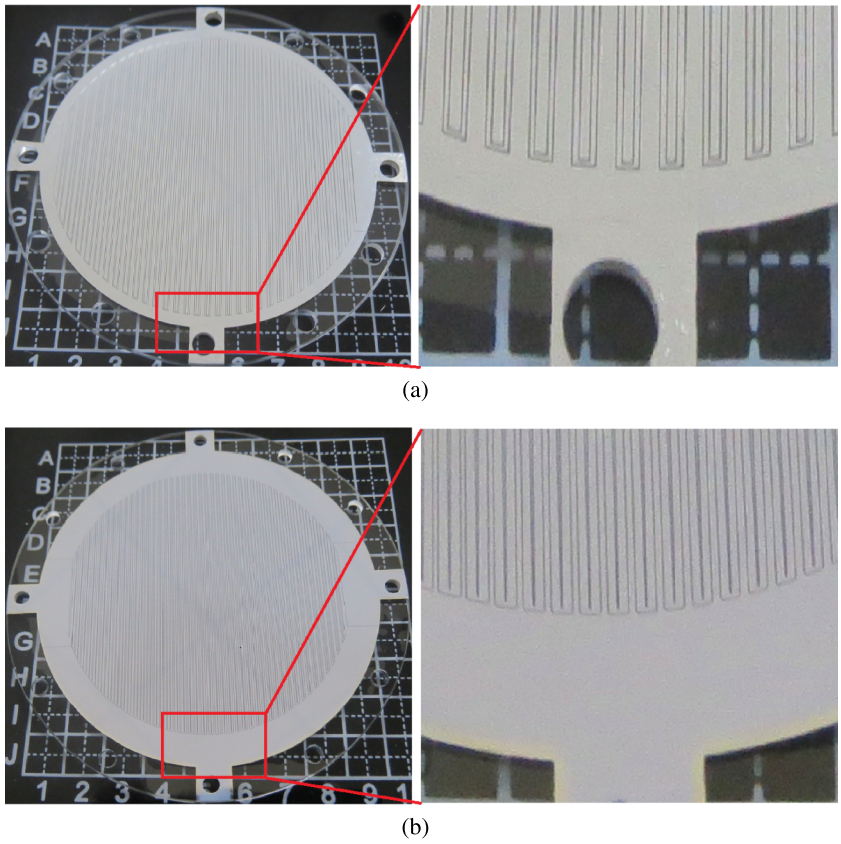

FIG. 8. Photographs of two round anodes fabricated by laser-micromachining method. (a) The WSA I. (b) The WSA II.

TABLE II. A comparison of the measured values with their calculated and simulated values for WSA I.

Capacitance (pF)	Z to S	Z to W	S to W
Measured capacitance	100.6	100.9	53.9
Simulated capacitance	123.23	123.41	60.78
Calculated capacitance	90.7	92.1	45.7
Simulated error (%)	22.50	22.31	12.76
Calculated error (%)	9.8	9.6	15.2

TABLE III. A comparison of the measured values with their calculated and simulated values for WSA II.

Capacitance (pF)	Z to S	Z to W	S to W
Measured value	137.4	138.3	68.9
Simulated capacitance	167.3	169.6	85.61
Calculated value	121.4	122.9	61.1
Simulated error (%)	21.76	22.63	24.25
Calculated error (%)	11.6	11.1	11.3

closer to the measured values. The calculated capacitances of $C_{total\text{-}ZS}$ and $C_{total\text{-}ZW}$ are about 11% less than those of the measured ones, and the error value of $C_{total\text{-}SW}$ is larger than that of $C_{total\text{-}ZS}$ and $C_{total\text{-}ZW}$ for the fabricated WSA. The main reason for this larger discrepancy for the calculated error value of $C_{total\text{-}SW}$ can be contributed to the fact that the capacitance coupling only exists between neighboring electrodes within the same period for the developed model here. According to the model, capacitance couplings between electrodes in different period and capacitances between W and S have been neglected, which has a greater influence on $C_{total\text{-}SW}$ than on $C_{total\text{-}ZS}$ and $C_{total\text{-}ZW}$ based on the WSA structure.

V. CONCLUSIONS

In summary, a novel model for calculating the WSA inter-electrode capacitance has been put forward. The calculated values of the inter-electrode capacitance are compared with experimental and simulated values for two round WSAs with different design parameters. It is found that there are about 9%–15% errors between the calculated values and measured ones, and the calculated capacitances obtained by our method are much closer to the measured values than those obtained by ANSYS software simulation. Based on our model, the optimized WSA structure is proposed for a less electronic noise and a better resolution. This model is useful for those who want to design a WSA or its transformation with small inter-electrode capacitances.

ACKNOWLEDGMENTS

The work is supported by the National Natural Science Foundation of China under Grant Nos. 61275152 and 61475154.

[1]Q. Ni, K. Song, S. Liu, L. He, B. Chen, and W. Yu, Opt. Express **23**, 30755 (2015).
[2]K. Werner and N. Kappelmann, 40th COSPAR Scientific Assembly, 2014.

[3]K. Werner, J. Barnstedt, W. Gringel, N. Kappelmann, H. Becker-Roß, S. Florek, R. Graue, D. Kampf, A. Reutlinger, C. Neumann, B. Shustov, A. Moisheev, and E. Skripunov, Adv. Space Res. **41**, 1992 (2008).
[4]J. Dong, B. T. Hu, Y. B. Chen, and Y. G. Xie, Chin. Phys. B **18**, 4229 (2009).
[5]Y. Tian, Y. G. Yang, Y. L. Li, and Y. J. L., Chin. Phys. C **37**, 056001 (2013).
[6]Y. Kanai, M. Hoshino, T. Kambara, T. Ikeda, and R. hellhammer, Nucl. Instrum. Methods Phys. Res., Sect. B **258**, 155 (2007).
[7]F. Gou, M. A. Gleeson, J. Villette, and A. W. Kleyn, Vacuum **81**, 196 (2006).
[8]D. Nandi, V. S. Prabhudesai, and E. Krishnakumar, Rev. Sci. Instrum. **76**, 053107 (2005).
[9]R. Grasso, S. Tudisco, A. Anzalone, F. Musumeci, A. Scordino, A. Sitaleri, R. Anzalone, G. D'Arrigo, and F. LaVia, Nucl. Instrum. Methods Phys. Res., Sect. A **720**, 122 (2013).
[10]Q. G. Tian, K. D. Wang, X. Shan, and X. J. Chen, Rev. Sci. Instrum. **82**, 033110 (2011).
[11]J. Yang, F. Wang, B. Xiao, X. Shan, and X. J. Chen, Chinese patent 104090290A (08 October 2014).
[12]C. G. Ning, X. G. Ren, and J. K. Deng, Chinese patent CN1553177 (08 December 2004).
[13]H. Yang, B. Zhao, Y. Liu, Q. Yan, and H. Hu, Rev. Sci. Instrum. **83**, 093107 (2012).
[14]Y. Wang, Y. Yang, X. Wang, and Y. Li, Nucl. Instrum. Methods Phys. Res., Sect. A **784**, 226 (2015).
[15]Y. Xing, B. Chen, H. F. Wang, H. J. Zhang, L. P. He, and F. Y. Jin, Acta Phys. Sin. **64**, 080702 (2015).
[16]J. R. Allington-Smith and H. E. Schwarz, Q. J. R. Astron. Soc. **25**, 267 (1984).
[17]J. Thornton, Nucl. Instrum. Methods Phys. Res., Sect. A **269**, 226 (1988).
[18]R. Igreja and C. J. Dias, Sens. Actuators, A **112**, 291 (2004).
[19]C. Ruan, L. Heng, and H. N. Liang, J. China Inst. Commun. **21**, 86 (2000).
[20]J. W. Brown and R. V. Churchill, *Complex variables and applications*, 6th ed. (McGraw-Hill, New York, 1996), Vol. 326.